

Onset of hard magnetic $L1_0$ FePt phase with (001) texture

An-Cheng Sun^{a,b}, Jen-Hwa Hsu^{a,b,*}, P.C. Kuo^c, H.L. Huang^{a,b}

^a Department of Physics, National Taiwan University, Taipei 106, Taiwan

^b Center for Nanostorage Research, National Taiwan University, Taipei 106, Taiwan

^c Institute of Materials Science and Engineering, National Taiwan University, Taipei 106, Taiwan

Received 4 September 2006; received in revised form 20 April 2007; accepted 13 June 2007

Available online 22 June 2007

Abstract

The perpendicular anisotropic magnetic properties of *in-situ* deposited FePt/Pt/Cr trilayer films were elucidated as functions of the deposition temperature and the sputtering rate of the FePt magnetic layer. Ordered $L1_0$ FePt thin films with perpendicular anisotropy and a (001) texture can be developed at a temperature as low as 300 °C with the sputtering of a FePt layer at a low rate. The larger Pt(001)[100] lattice induced an expansion of the FePt *a*- and *b*-axis, leading to the contraction of the FePt *c*-axis, enabling the epitaxial growth of the $L1_0$ FePt(001) texture to occur. A low rate of sputtering of the FePt thin film promotes the formation of the magnetically hard FePt(001) texture on the surface of the Pt(001) buffer layer at low temperature, while the high sputtering rate of FePt layer suppresses the phase transformation.

© 2007 Elsevier B.V. All rights reserved.

Keywords: FePt thin films; Anisotropy; Magnetic properties and measurements; Phase transitions; Sputtering

1. Introduction

Investigations of the $L1_0$ FePt film have begun to focus on its perpendicular magnetic anisotropy, which is required to fulfill the requirements of magnetic perpendicular recording. The crystalline anisotropy of $L1_0$ FePt ($K_u \sim 10^7$ J/m³) is at least one order of magnitude greater than that of Co-based materials ($K_u \sim 2 \times 10^5$ J/m³) [1]. Therefore, small $L1_0$ FePt grains such as those of size 2.8 nm can also have high thermal stability [1]. The desired preferred orientation of the $L1_0$ FePt film must be (001), making the magnetic easy axis ([001]-axis) perpendicular to the film plane and enabling the thin $L1_0$ FePt film to be used as the perpendicular recording medium. In earlier studies, the FePt(001) preferred orientation was obtained using the epitaxial method, but the ordering temperature normally exceeded 450 °C [2–5], causing grain growth [2,6,7] and interlayer diffusion [8,9]. Accordingly, developing an effective scheme for preparing the $L1_0$ FePt(001) film with perpendicular magnetic anisotropy at low temperatures is of priority concern.

Efforts have been made to reduce the ordering temperature of the $L1_0$ FePt thin film. For instance, the formation of excess defects such as vacancies [6,10], solutes [11], and inclusions [12] has been proposed. In these approaches, the energy barrier to the order–disorder transformation of the FePt phase was reduced and the ordering temperature of the $L1_0$ FePt phase can be thus lowered to less than 400 °C. However, the preferred orientation of FePt is FePt(111). Recently, Lai et al. further reduced the ordering temperature of $L1_0$ FePt to 275 °C [13]. In their process, a Cu underlayer on the HF-cleaned Si(001) substrate underwent postannealing at 275 °C. During the formation of copper silicide Cu₃Si upon postannealing, the expansion in volume induced a dynamic in-plane tensile stress in the FePt films, facilitating the formation of the ordered FePt phase at low temperatures. Although a low ordering temperature can be thus achieved, this approach also only yielded the FePt (111) phase. This article presents an effective method of preparing an $L1_0$ FePt(001) film with perpendicular magnetic anisotropy at low temperatures. Such a film was epitaxially grown on Pt(001)/Cr(002) bilayer film. The Pt(001) lattice induces an in-plane tensile stress in the FePt(001) plane, expanding the *a*- and *b*-axis of FePt, causing the contraction of the *c*-axis. The onset of the ordered $L1_0$ FePt(001) texture

* Corresponding author. Department of Physics, National Taiwan University, Taipei 106, Taiwan. Tel.: +886 2 33665162; fax: +886 2 33665892.

E-mail address: jhhsu@phys.ntu.edu.tw (J.-H. Hsu).

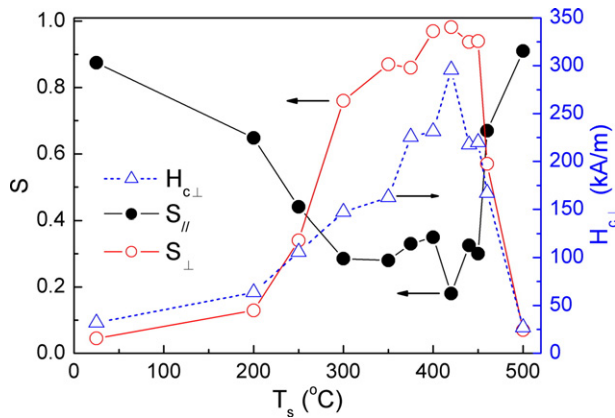


Fig. 1. The squareness ($S=M_r/M_s$) and the out-of-plane coercivity ($H_{c\perp}$) of FePt/Pt/Cr trilayer films as a function of deposition temperature T_s of FePt magnetic layer.

occurs at a temperature as low as 300 °C. This fact promotes the use of an FePt thin film in the magnetic recording industry.

2. Experiments

Fe₄₈Pt₅₂ thin films with the structure FePt(20 nm)/Pt(2 nm)/Cr(90 nm)/7059 coming glass, were fabricated by conventional direct-current magnetron sputtering in an ultra-high vacuum sputtering chamber. The base pressure was under 2.7×10^{-7} Pa before sputtering. The working pressure of Cr underlayer and a Pt buffer layer were fixed at 0.667 and 1.333 Pa and the sputtering rates were set at 0.0321 and 0.005 nm/s, respectively. The substrate was maintained at 350 °C to deposit a Cr underlayer and a Pt buffer layer. At these sputtering conditions, the Cr underlayer and the Pt buffer layer grew with (002) and (001) plane textures, respectively. Next, the FePt magnetic layer was deposited on a Pt(001) plane. The deposition temperature of the FePt layer (T_s) was varied from room temperature to 500 °C, and the sputtering rate (R) was varied from 0.0085 to 0.0300 nm/s. The sputtering rate of the FePt layer, 0.0085 nm/s, is the lowest one attainable in our system herein with the stable plasma. The film thickness was determined using an atomic force microscope. The crystal structures of the films were examined by X-ray diffraction (XRD) using Cu-K α radiation. The magnetic properties were measured using a vibrating sample magnetometer at room temperature with a maximum applied field of $\sim 10^3$ kA/m. The interfacial microstructure was investigated using a 300 keV high-resolution transmission electron microscope (HRTEM).

3. Results and discussion

3.1. Effects of deposition temperatures on structures and magnetic properties of FePt magnetic layer

Fig. 1 plots the squareness ($S=M_r/M_s$) and the out-of-plane coercivity ($H_{c\perp}$) of FePt/Pt/Cr trilayer films as functions of the deposition temperature of the FePt magnetic layer. The sputtering rate R was 0.0085 nm/s. The in-plane squareness (S_{\parallel}) considerably exceeded the out-of-plane squareness (S_{\perp}) when T_s was lower than 200 °C. As T_s was increased from 200

to 300 °C, S_{\parallel} substantially declined, and S_{\perp} increased markedly. $S_{\perp}=0.75$ and $S_{\parallel}=0.28$ when $T_s=300$ °C, revealing that the magnetic anisotropy had switched from in-plane to out-of-plane in the FePt/Pt/Cr trilayer films. When T_s was in the range 300 and 450 °C, S_{\perp} always exceeded 0.85 whereas S_{\parallel} was less than 0.4. Additionally, the out-of-plane coercivity ($H_{c\perp}$) also depended on T_s , as presented in Fig. 1. $H_{c\perp}$ was less than 60 kA/m when $T_s < 200$ °C. As T_s was increased from 200 to 300 °C, $H_{c\perp}$ rose greatly from 64 to 143 kA/m. The largest value of $H_{c\perp}$ was around 294.5 kA/m and was measured at $T_s=420$ °C. S_{\perp} of this film was close to one. However, at $T_s > 460$ °C, $H_{c\perp}$ substantially decreased with a large drop in S_{\perp} .

Fig. 2 displays the XRD patterns of FePt/Pt/Cr trilayer films at various T_s of the FePt layer with R set to 0.0085 nm/s. As shown in Fig. 2, a strong Cr(002) peak was always present. When the Pt layer was grown on the Cr(002) plane, the Pt(001) [100] could grow epitaxially along Cr(002)[110]. However, identifying the Pt(001) peak in the XRD pattern in our trilayer system is difficult, because the thickness of the Pt buffer layer is only 2 nm — too thin to be detected by XRD. Accordingly, the peak of Pt(001) is very small and hardly visible. However, T_s strongly affected the orientation of the FePt layer when FePt was deposited onto the Pt(001) plane at various T_s . The fcc FePt (200) peak appeared when $T_s=200$ °C. The ordered $L1_0$ FePt (001) peak began to develop as T_s was increased to 250 °C. A broad peak that was the superposition of the fcc FePt(200) and $L1_0$ FePt(002) peaks appeared between 45° and 50°, shifting to higher angles as T_s was increased. It is a single and sharp $L1_0$ FePt(002) peak at $T_s \sim 440$ °C.

Fig. 3 plots the integrated intensities, the peak positions of the FePt(001) and (002) peaks, the ordering parameter (S_{order}) and the c -axis parameter of FePt as functions of T_s . The intensities of the FePt(001) and (002) peaks were integrated with the Gaussian function. In Fig. 3(a), the integrated intensity of FePt(002) greatly exceeded that of FePt(001) at $T_s=250$ °C. As T_s was increased from 250 to 300 °C, the integrated intensity of FePt(002) decreased drastically. A rapid decline in the integrated intensity also occurred when $T_s > 450$ °C. Above this temperature, the integrated intensities of both FePt(001) and

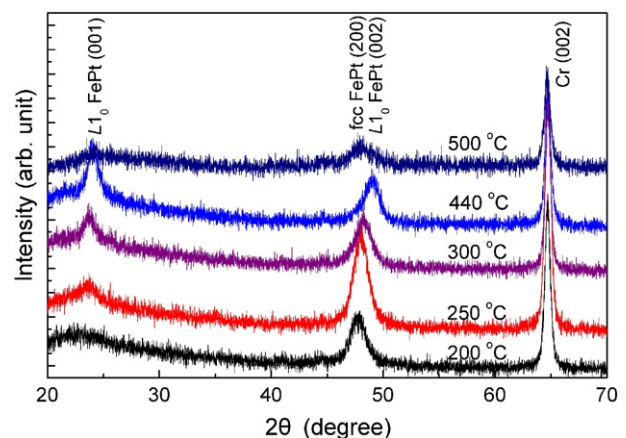


Fig. 2. XRD patterns of FePt/Pt/Cr trilayer films with various deposition temperatures T_s of FePt magnetic layer.

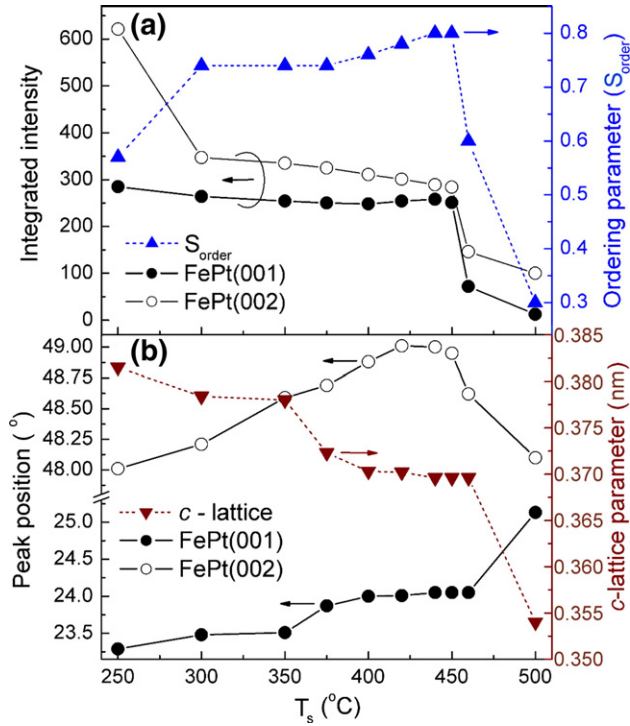


Fig. 3. Dependence of (a) the integrated intensities of FePt(001) as well as (002) peaks and ordering parameter (S_{order}) and (b) the positions of FePt(001) as well as (002) peaks and c -lattice parameter of FePt on the deposition temperature T_s of the FePt layer.

(002) fell substantially. The ordering parameter (S_{order}) was obtained from the following formula [14]. Fig. 3(a) plots the results as a function of T_s .

$$S_{order} = \left[\left(\frac{I_{001}}{I_{002}} \right) \times \left(\frac{F_f}{F_s} \right)^2 \times \frac{(L \times A \times D)_f}{(L \times A \times D)_s} \right]^{1/2} \quad (1)$$

$$\cong 0.85 \times \left(\frac{I_{001}}{I_{002}} \right)^{1/2}$$

where I_{001} and I_{002} represent the integrated intensities of the (001) and (002) peaks, respectively. Where F denotes the structural factor; L is the Lorentz polarization factor; A is the absorption factor; D is the temperature factor, and the subscripts f and s refer to the fundamental and superlattice peaks, respectively. As shown in Fig. 3(a), S_{order} increased markedly with the temperature from 250 to 300 °C, and then remained between 0.75 and 0.8 as T_s rose further from 300 to 450 °C. S_{order} then decreased rapidly as T_s increased further. Fig. 3(b) plots the peak positions of FePt(001) and (002), and the c -lattice parameter at various T_s . The superlattice FePt(001), (002) and fundamental FePt(200) for bulk FePt were present at 23.97°, 49.04° and 47.62°, respectively. In Fig. 3(b), both FePt(001) and (002) peak positions moved to higher angles gradually as T_s was increased from 250 to 450 °C. The FePt(001) and (002) peak positions reached the bulk values of FePt as T_s was increased to 420 °C. At this temperature, a maximum value of $H_{c\perp}$ was obtained, as described earlier. Fig. 3(b) presents the calculated d -spacings of the FePt(001) planes (c -lattice

parameter), $d_{FePt(001)}$, according to the Bragg law [15]. The fundamental and superlattice d -spacings of FePt(001) are 0.382 and 0.372 nm, respectively. The c -lattice parameter was contracted to 0.3784 nm when $T_s=300$ °C. Further increasing T_s promotes the shrinkage of the c -lattice parameter.

The soft magnetic FePt phase has a face-centered cubic structure with $a=b=c=0.382$ nm, whereas the hard magnetic $L1_0$ FePt phase has a face-centered tetragonal (fct) structure with $a=b=0.386$ nm and $c=0.372$ nm. The c -axis of the ordered FePt is also the magnetic easy axis [001]. When the order–disorder transformation occurs, the fcc FePt transforms to fct FePt. In the FePt/Pt/Cr trilayer films herein, the Pt(001) [100] in-plane axis is 1.6 % larger than the FePt(001)[100] in-plane axis. When the FePt layer is stacked on the Pt(001)/Cr (002) bilayer film, the Pt lattice will elongate the in-plane axes of FePt. The expansion of the a - and b -axis of FePt results in the contraction of the c -axis of FePt, and the consequent formation of the ordered FePt(001) phase [2,8]. Therefore, when $T_s=300$ °C, Fe and Pt atoms acquired sufficient energy to diffuse over a long distance to the lattice sites of the Pt(001) surface, such that the FePt(001) plane was well developed (Fig. 2). Accordingly, S_{\perp} greatly exceeded S_{\parallel} , and perpendicular magnetic anisotropy was achieved. However, at $T_s < 300$ °C, Fe and Pt atoms without sufficient energy could not move to the lattice sites of Pt(001) surface, so the disordered FePt phase was formed in the FePt/Pt/Cr trilayer film. This result demonstrates that the onset of the ordered FePt(001) texture in our trilayer structure occurs at a temperature as low as 300 °C. Additionally, the hard magnetism was destroyed at high temperatures of over, say, 460 °C, by the diffusion of Cr atoms into the FePt layer [9].

3.2. Effects of sputtering rates on structures and magnetic properties of FePt magnetic layer

The epitaxial growth of thin films primarily depends upon the diffusion time as well as diffusion distance and both depend on the sputtering rate R [16–18]. Therefore in order to investigate effect of R on the formation of the FePt(001) plane,

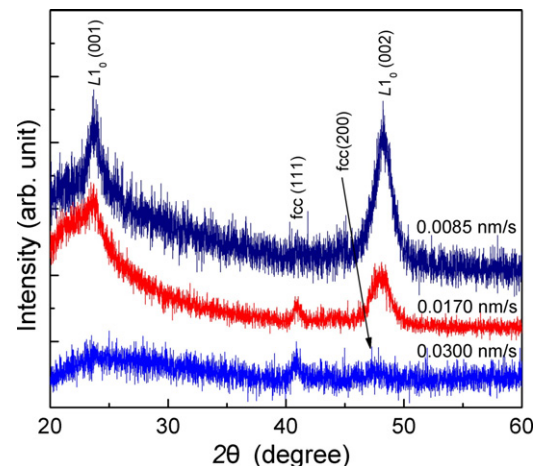


Fig. 4. XRD patterns of FePt/Pt/Cr trilayer films with various sputtering rates R of FePt magnetic layer. The FePt layer was deposited at 300 °C.

various R of the FePt layer were employed to prepare FePt/Pt/Cr trilayers at $T_s=300$ °C. Fig. 4 displays XRD patterns of FePt/Pt/Cr trilayer films obtained with three different R . The disordered soft fcc FePt(111) peak appeared when $R=0.03$ nm/s. The ordered $L1_0$ FePt(001) peak was not observed. As R was reduced to 0.017 nm/s, the fcc FePt(200), $L1_0$ FePt(001) and $L1_0$ FePt(002) peaks were present simultaneously. However, as R was reduced further to 0.0085 nm/s, the intensity of the $L1_0$ FePt(001) peak increased considerably and the position of the peak between 45° and 50° was close to that of the $L1_0$ FePt(002) peak. Fig. 5 plots the perpendicular hysteresis loops of the FePt/Pt/Cr trilayer film with three different R . $M_{r\perp}$ was the highest at a sputtering rate of FePt 0.0085 nm/s, while $M_{r\perp}$ was the lowest at the highest sputtering rate of the FePt layer. Consequently, S_\perp was higher at a lower FePt sputtering rate. Furthermore, $H_{c\perp}$ fell from 149 to 96 kA/m as R was increased from 0.0085 to 0.03 nm/s, indicating that the small R promotes the formation of the perpendicular magnetically hard $L1_0$ FePt(001) film.

From above results, the FePt(001) phase can epitaxially grow on the Pt(001)/Cr(002) bilayer film at 300 °C only when $R=0.0085$ nm/s. At this rate, Fe and Pt atoms have sufficient time to diffuse to the positions of the local free energy minimum on the Pt(001) plane, forming the equilibrium ordered FePt(001) structure. However, the deposition time decreases as R increases. Therefore, at a high rate of 0.03 nm/s, the Fe and Pt atoms do not have sufficient time to finish the diffusion. The probability of an encounter between the migrating atoms and the atoms of Pt(001) plane becomes very low, resulting in the formation of the disordered and soft magnetic FePt phase.

Fig. 6 presents the cross sectional TEM bright field image of the FePt/Pt/Cr trilayer film. The sputtering rate and deposition temperature of FePt were 0.0085 nm/s and 300 °C, respectively. In Fig. 6(a), epitaxial growth was initiated from the Cr(002) underlayer, continued through the Pt(001) buffer layer, and extended into the FePt(001) magnetic layer. Fig. 6(b) presents the magnified image of the dashed-square portion in Fig. 6(a). The value of $d_{\text{FePt}(001)}$ calculated from Fig. 6(b) was 0.379 nm. This value is consistent with the results of XRD displayed in

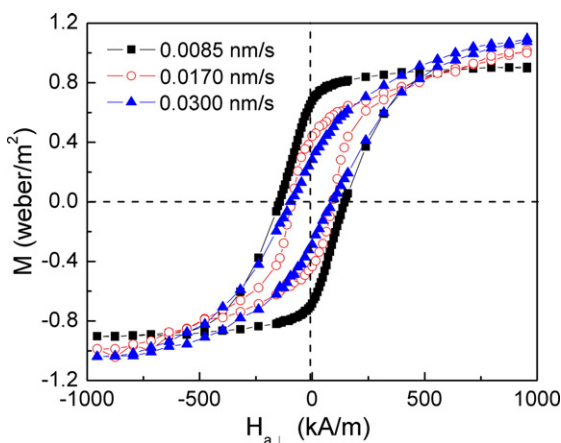


Fig. 5. The perpendicular hysteresis loops of FePt/Pt/Cr trilayer films, with various sputtering rates R of FePt magnetic layer. The FePt layer was deposited at 300 °C.

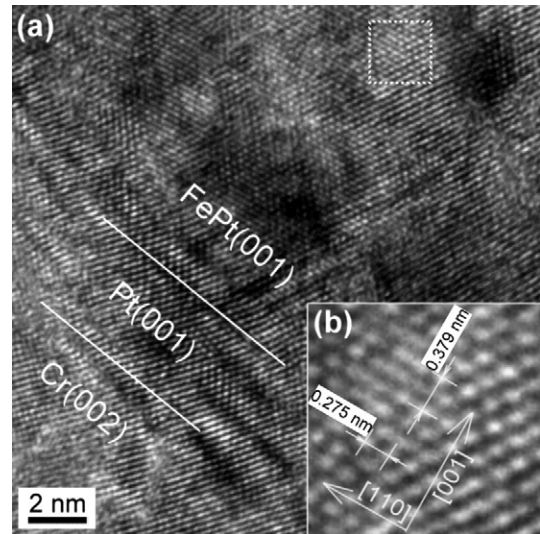


Fig. 6. Cross sectional TEM bright field image of FePt/Pt/Cr trilayer film. The sputtering rate R and deposition temperature T_s of FePt were 0.0085 nm/s and 300 °C, respectively.

Fig. 3(b). However, the value of $d_{\text{FePt}(110)}$ calculated from Fig. 6 (b) is 0.275 nm, giving $d_{\text{FePt}(100)}$ and $d_{\text{FePt}(010)}$ values of both 0.389 nm. This value exceeds that, 0.386 nm, of bulk $L1_0$ FePt. This result indicates that the a - and b -axes of $L1_0$ FePt were enlarged to 0.389 nm by the Pt(001) lattice at 300 °C, simultaneously reducing the c -axis of the $L1_0$ FePt phase. Accordingly, the temperature of the onset of ordering of $L1_0$ FePt was reduced from 500 °C to 300 °C.

4. Conclusion

The ordered $L1_0$ FePt(001) texture with perpendicular magnetic anisotropy was prepared on a Pt(001)/Cr(002) bilayer film at a low ordering temperature and at a low FePt sputtering rate. When the deposition temperature of the FePt layer reached 300 °C, a high out-of-plane squareness with a (001) $L1_0$ FePt film texture was obtained. The Pt(001) buffer layer expanded the a - and b -axis of FePt(001) and contracted the c -axis. The FePt(001) texture was thus developed on the Pt(001) film plane. The $L1_0$ FePt(001) texture is expected to be able to be obtained at a temperature that is much lower than 300 °C when the sputtering rate of FePt layer is less than 0.0085 nm/s.

Acknowledgments

The authors would like to thank the Ministry of Economic Affairs of Taiwan for financially supporting this research under Contract No. MOEA94-EC-17-A-08-S1-0006.

References

- [1] D. Weller, A. Moser, L. Folks, M.E. Best, W. Lee, M.F. Toney, M. Schwickert, J.U. Thiele, M.F. Doerner, IEEE Trans. Magn. 36 (2000) 10.
- [2] Y.K. Takahashi, K. Hono, T. Shima, K. Takanashi, J. Magn. Magn. Mater. 267 (2003) 248.
- [3] S. Jeong, T. Ohkubo, A.G. Roy, D.E. Laughlin, M.E. McHenry, J. Appl. Phys. 91 (2002) 6863.

- [4] T. Suzuki, K. Harada, N. Honda, K. Ouchi, *J. Magn. Magn. Mater.* 193 (1999) 85.
- [5] E.B. Svedberg, J.J. Mallett, S. Sayan, A.J. Shapiro, W.F. Egelhoff Jr., T. Moffat, *Appl. Phys. Lett.* 85 (2004) 1353.
- [6] A.C. Sun, P.C. Kuo, S.C. Chen, C.Y. Chou, H.W. Chang, J.-H. Hsu, H.L. Huang, *IEEE Trans. Magn.* 41 (2005) 3772.
- [7] A.C. Sun, P.C. Kuo, S.C. Chen, C.Y. Chou, H.L. Huang, J.-H. Hsu, *J. Appl. Phys.* 95 (2004) 7264.
- [8] J.S. Chen, Y. Xu, J.P. Wang, *J. Appl. Phys.* 93 (2003) 1661.
- [9] A.C. Sun, P.C. Kuo, J.-H. Hsu, H.L. Huang, J.M. Sun, *J. Appl. Phys.* 98 (2005) 076109.
- [10] C.H. Lai, C.H. Yang, C.C. Chiang, *Appl. Phys. Lett.* 83 (2003) 4550.
- [11] T. Maeda, T. Kai, A. Kikitsu, T. Nagase, J. Akiyama, *Appl. Phys. Lett.* 80 (2002) 2147.
- [12] K. Leistner, J. Thomas, H. Schlörb, M. Weisheit, L. Schultz, S. Fähler, *Appl. Phys. Lett.* 85 (2004) 3498.
- [13] C.H. Lai, C.H. Yang, C.C. Chiang, T. Balaji, T.K. Tseng, *Appl. Phys. Lett.* 85 (2004) 4430.
- [14] J.A. Christodoulides, P. Farber, M. Daniil, H. Okumura, G.C. Hadjipanayis, V. Simopoulos, D. Waller, *IEEE Trans. Magn.* 37 (2001) 1292.
- [15] B.D. Cullity, *Elements of X-ray Diffraction*, Addison Wesley, Reading, MA, 1978.
- [16] S. Nakagawa, T. Kamiki, *J. Magn. Magn. Mater.* 287 (2005) 204.
- [17] T.D. Khoa, S. Horii, S. Horita, *Thin Solid Films* 419 (2002) 88.
- [18] J.D. Suh, G.Y. Sung, K.Y. Kang, *IEEE Trans. Magn.* 9 (1999) 1708.